Journal of Organometallic Chemistry 694 (2009) 2328–2335

Contents lists available at ScienceDirect

Journal of Organometallic Chemistry

journal homepage: www.elsevier.com/locate/jorganchem

Design of nickel chelates of tetradentate N-heterocyclic carbenes with subdued cytotoxicity

Sriparna Ray [a], Jayant Asthana [b], Joseph M. Tanski [c], Mobin M. Shaikh [d], Dulal Panda [b,*], Prasenjit Ghosh [a,*]

[a] Department of Chemistry, Indian Institute of Technology Bombay, Powai, Mumbai 400 076, India
[b] School of Biosciences and Bioengineering, Indian Institute of Technology Bombay, Powai, Mumbai 400 076, India
[c] Department of Chemistry, Vassar College, 124 Raymond Avenue, Poughkeepsie, NY-12604, United States
[d] National Single Crystal X-ray Diffraction Facility, Indian Institute of Technology Bombay, Powai, Mumbai 400 076, India

ARTICLE INFO

Article history:
Received 4 February 2009
Received in revised form 17 March 2009
Accepted 19 March 2009
Available online 27 March 2009

Keywords:
Nickel
N-heterocyclic carbene
Cytotoxicity
Chelation
DFT studies

ABSTRACT

A series of nickel complexes, **1b**–**3b**, exhibiting subdued cytotoxicity have been designed with the intent of their use as agents for developing resistance to nickel toxicity. Indeed, the nickel complexes, **1b**–**3b**, display less cytotoxic activity towards two commonly occurring human cancer cell lines namely, HeLa cells (16–64%) and MCF-7 cells (70–90%) in culture as compared to the maximum inhibition by $NiCl_2 \cdot 6H_2O$ under analogous conditions at three different concentrations (1 μM, 5 μM and 20 μM). Similarly, the suppression of cytotoxicity through chelation of the metal ion can also be seen in normal cells as was evident from a significant reduction in cytotoxicity (9–41%) for a non-tumorigenic CHO cell line in case of a representative complex **3b**. The reduction in carcinogenic activity in the complexes relative to nickel(II) ion from $NiCl_2 \cdot 6H_2O$ is brought about by successful chelation of the metal center by a class of specially designed new tetradentate *N*/*O*-functionalized N-heterocyclic carbene ligands. The two strongly σ-donating carbene moieties coupled with two negatively charged amido moieties present in the N-heterocyclic carbene ligands facilitate complete chelation of the metal center and thereby significantly reduce the cytotoxic effects of the metal.

1. Introduction

The day-to-day exposure to metals, including some very toxic ones like nickel, in varied amounts in occupational as well as in environmental settings pose a grave risk to public health in the modern era [1]. In this context, of particular relevance is nickel, which is a well-established human carcinogen that is frequently encountered in workplace and its surrounding environment and arise from its association with several important industrial processes that range from nickel mining and refining to electroplating to the production of much popular Ni–Cd batteries to the combustion of fossil fuels to the incineration of nickel-containing solid waste, etc. [2]. Furthermore, the release of nickel in the environment also contributes to significant non-occupational exposure [3].

The counter strategy to thwart this menace involves reducing the cytotoxicity of the metal center by chelation with strongly binding ligands [4]. For example, this strategy has been successfully used for gadolinium, which by itself is extremely toxic, but when chelated with appropriate ligands, it exhibits subdued cytotoxicity and have been routinely used in radiotherapy for treatment of cancers [5]. A common methodology employed to develop resistance towards any useful but toxic metal, is the gradual exposure to a minute amount of the complex of the same metal. Such investigations are being successfully carried out in cases of nickel [6] and cadmium [7].

Of late, there has been an interest in developing the chemistry of nickel complexes of N-heterocyclic carbene ligands, resulting in the synthesis of several such complexes supported over a wide variety of the NHC ligands. Quite a few applications of these Ni–NHC complexes have also been reported ranging from Suzuki cross coupling [8] to C–C and C–F activation [9] to olefin polymerization [10] to aryl Grignard cross coupling [11] to Heck reaction [12], etc. As the biomedical studies of the Ni–NHC complexes have not yet been carried out, we became interested in exploring this area.

In this regard, our approach focuses on designing nickel compounds with significantly reduced carcinogenic activities for their potential applications in developing resistance to nickel toxicity. In particular, we planned to diminish the carcinogenic activity of the metal, as compared to its ionic state, Ni^{2+}, by engulfing the metal through appropriate ligation. As our interest lies in exploring the utility of non-functionalized and *N*/*O*-functionalized N-heterocyclic carbenes [13] in biomedical applications [14] and in chemical catalysis [15] we chose to employ suitably tailored *N*/*O*-functionalized N-heterocylic carbene ligands for designing these

* Corresponding author. Tel.: +91 22 2576 7178; fax: +91 22 2572 3480.
E-mail addresses: panda@iitb.ac.in (D. Panda), pghosh@chem.iitb.ac.in (P. Ghosh).

0022-328X/$ - see front matter © 2009 Elsevier B.V. All rights reserved.
doi:10.1016/j.jorganchem.2009.03.036

nickel complexes with reduced carcinogenic activities. Furthermore, keeping the subdued cytotoxic activity in mind, we also planned in making these nickel complexes water soluble by putting polar functional groups as N-substituents on the N-heterocylic carbene ligands.

Here, in this contribution, we report a series of nickel complexes namely, {*N,N′-bis*-{[2-(1-R)-imidazol-2-ylidene]acetyl}ethylenediamine}Ni [R = Me (**1b**), *i*Pr (**2b**), CH_2Ph (**3b**)], which are completely engulfed by a class of *N*/*O*-functionalized N-heterocylic carbene ligands and which show significantly reduced cytotoxicity with respect to $NiCl_2 \cdot 6H_2O$ and therefore are of interest as potential agents for developing resistance towards nickel cytotoxicity (Fig. 1).

2. Experimental

2.1. General procedures

All manipulations were carried out using a combination of a glovebox and standard Schlenk techniques. Solvents were purified and degassed by standard procedures. $NiCl_2 \cdot 6H_2O$ was purchased from SD-fine Chemicals (India) and 1-methylimidazole was purchased from Spectrochem Pvt. Ltd. (Mumbai, India) and were used without further purification. The 1-*i*-propylimidazole [16] and 1-benzylimidazole [17] were prepared according to the literature procedures. ^1H and $^{13}C\{^1H\}$ NMR spectra were recorded on a Varian 400 MHz NMR spectrometer. ^1H NMR peaks are labeled as singlet (s), doublet (d), triplet (t), multiplet (m), and septet (sept). Infrared spectra were recorded on a Perkin–Elmer Spectrum One FT-IR spectrometer. X-ray diffraction data for **1b** were collected on an Oxford Diffraction Excaliber-S diffractometer while **2b** and **3b** were collected on a Bruker APEX 2 CCD platform diffractometer. The crystal data collection and refinement parameters are summarized in Table S1 (Supplementary Supporting Information). The structures were solved using direct methods and standard difference map techniques, and were refined by full-matrix least-squares procedures on F^2 with SHELXTL (Version 6.10) [18].

2.2. N,N′-bis-{[2-(1-methyl)-imidazolium]acetyl}ethylenediamine dichloride (*1a*)

N,N′-bis-(2-chloroacetyl)ethylenediamine (1.07 g, 5.02 mmol) and 1-methylimidazole (0.823 g, 10.0 mmol) were taken in toluene (*ca.* 10 mL) and refluxed overnight to obtain a light brown precipitate, which was isolated by decanting off the solvent. The residue was washed with hot hexane (*ca.* 15 mL) and dried under vacuum to obtain the product **1a** as a light brown powder (1.03 g, 55%). ^1H NMR (DMSO-d_6, 400 MHz, 25 °C): δ 9.20 (s, 2H, NC*H*N), 9.01 (br, 2H, N*H*), 7.74 (s, 2H, NC*H*CHN), 7.70 (s, 2H, NCHC*H*N), 5.04 (s, 4H, CH_2), 3.88 (s, 6H, CH_3), 3.20 (s, 4H, CH_2). $^{13}C\{^1H\}$ NMR (DMSO-d_6, 100 MHz, 25 °C): δ 165.2 (*C*O), 137.6 (N*C*N), 123.6 (N*C*HCHN), 123.0 (NCH*C*HN), 50.6 (*C*H_2), 38.3 (*C*H_2), 35.7 (*C*H_3). IR data (KBr pellet cm^{-1}): 3456 (s), 3226 (w), 3153 (w), 3073 (m), 2942 (w), 2860 (w), 2059 (w), 1681 (s), 1565 (s), 1439 (m), 1379 (m), 1262 (m), 1177 (s), 1086 (m), 1030 (w), 968 (w), 847 (w), 763 (m), 704 (w), 666 (w), 623 (m), 564 (w). HRMS (ES): *m*/*z* 305.1725 $[(NHC)\text{-}H]^+$, Calculated 305.1726.

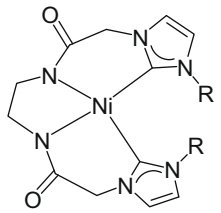

R = Me (**1b**), *i*Pr (**2b**), CH_2Ph (**3b**)

Fig. 1. Ligand encapsulated nickel complexes, **1b**–**3b**.

2.3. {N,N′-bis-{[2-(1-methyl)-imidazol-2-ylidene]acetyl} ethylenediamine}Ni (*1b*)

N,N′-bis-{[2-(1-methyl)-imidazolium]acetyl}ethylenediamine dichloride (0.377 g, 1.00 mmol), $NiCl_2 \cdot 6H_2O$ (0.237 g, 1.00 mmol) and K_2CO_3 (0.417 g, 3.02 mmol) were taken in CH_3CN (*ca.* 30 mL). The reaction mixture was refluxed for 24 h, filtered and the solvent was removed. The residue was extracted in CH_2Cl_2, (*ca.* 20 mL) which was evaporated under vacuum to obtain the product **1b** as a yellow solid (0.237 g, 66%). Single crystal of **1b** was grown by slow evaporation method from a saturated CH_3CN solution. ^1H NMR (CD_3OD, 400 MHz, 25 °C): δ 7.27 (d, $^3J_{H-H}$ = 2 Hz, 2H, NC*H*CHN), 7.15 (d, $^3J_{H-H}$ = 2 Hz, 2H, NCHC*H*N), 5.06 (d, $^2J_{H-H}$ = 16 Hz, 2H, CH_2), 4.48 (d, $^2J_{H-H}$ = 16 Hz, 2H, CH_2), 3.88 (d, $^3J_{H-H}$ = 7 Hz, 2H, CH_2), 3.21 (s, 6H, CH_3), 2.36 (d, $^3J_{H-H}$ = 7 Hz, 2H, CH_2). $^{13}C\{^1H\}$ NMR (CD_3OD, 100 MHz, 25 °C): δ 168.9 (*C*O), 166.7 (N*C*N–Ni), 124.5 (N*C*HCHN), 123.3 (NCH*C*HN), 55.3 (*C*H_2), 48.4 (*C*H_2), 37.1 (*C*H_3). IR data (KBr pellet cm^{-1}): 3434 (m), 2853 (w), 1575 (s), 1495 (s), 1454 (m), 1403 (m), 1293 (m), 1249 (s), 1204 (m), 1167 (w), 1090 (w), 960 (w), 803(m), 755 (w), 719 (w), 702 (m), 674 (w), 609 (w), 459 (w). HRMS (ES): *m*/*z* 361.0911 $[(NHC)Ni+H]^+$, Calculated 361.0923. Anal. Calc. for $C_{14}H_{18}N_6NiO_2 \cdot H_2O$ (379.04): C, 44.36; H, 5.32; N, 22.17. Found: C, 44.13; H, 5.14; N, 22.17%.

2.4. N,N′-bis-{[2-(1-i-propyl)-imidazolium]acetyl}ethylenediamine dichloride (*2a*)

N,N′-bis-(2-chloroacetyl)ethylenediamine (1.07 g, 5.02 mmol) and 1-*i*-propylimidazole (1.10 g, 10.0 mmol) were taken in toluene (*ca.* 10 mL) and refluxed overnight to obtain a light brown precipitate, which was isolated by decanting off the solvent. The residue was washed with hot hexane (*ca.* 15 mL) and dried under vacuum to obtain the product **2a** as a light brown powder (1.48 g, 68%). ^1H NMR (DMSO-d_6, 400 MHz, 25 °C): δ 9.44 (s, 2H, NC*H*N), 9.00 (br, 2H, N*H*), 7.92 (s, 2H, NC*H*CHN), 7.79 (s, 2H, NCHC*H*N), 5.06 (s, 4H, CH_2), 4.68 (sept, $^3J_{H-H}$ = 8 Hz, 2H, C*H*$(CH_3)_2$), 3.20 (s, 4H, CH_2), 1.47 (d, $^3J_{H-H}$ = 8 Hz, 12H, CH(CH_3)$_2$). $^{13}C\{^1H\}$ NMR (DMSO-d_6, 100 MHz, 25 °C): δ 165.3 (*C*O), 136.0 (N*C*N), 123.9 (N*C*HCHN), 120.0 (NCH*C*HN), 52.3 (*C*H$(CH_3)_2$), 50.7 (*C*H_2), 38.3 (*C*H_2), 22.3 (CH(*C*H_3)$_2$). IR data (KBr pellet cm^{-1}): 2985 (s), 2054 (w), 1682 (s), 1564 (m), 1513 (m), 1466 (w), 1432 (w), 1377 (w), 1349 (w), 1299 (w), 1261 (w), 1182 (m), 1085(w), 1036 (m), 1008 (m), 819 (w), 761 (w), 693 (w), 658 (w), 624 (w), 577 (w). HRMS (ES): *m*/*z* 361.2348 $[(NHC)\text{-}H]^+$, Calculated 361.2352.

2.5. {N,N′-bis-{[2-(1-i-propyl)-imidazol-2-ylidene]acetyl} ethylenediamine}Ni (*2b*)

N,N′-bis-{[2-(1-*i*-propyl)-imidazolium]acetyl}ethylenediamine dichloride (0.433 g, 1.00 mmol), $NiCl_2 \cdot 6H_2O$ (0.237 g, 1.00 mmol) and K_2CO_3 (0.417 g, 3.02 mmol) were taken in CH_3CN (*ca.* 30 mL). The reaction mixture was refluxed for 24 h, filtered and the solvent was removed. The residue was extracted in CH_2Cl_2, (*ca.* 20 mL) which was evaporated under vacuum to obtain the product **2b** as a yellow solid (0.268 g, 64%). Single crystal of **2b** was grown by slow evaporation method from a saturated CH_3CN solution. ^1H NMR ($CDCl_3$, 400 MHz, 25 °C): δ 6.98 (br, 2H, NC*H*CHN), 6.91 (br, 2H, NCHC*H*N), 4.95 (d, $^2J_{H-H}$ = 15 Hz, 2H, CH_2), 4.47 (d, $^2J_{H-H}$ = 15 Hz, 2H, CH_2), 3.93 (d, $^3J_{H-H}$ = 7 Hz, 2H, CH_2), 3.79 (sept, $^3J_{H-H}$ = 7 Hz, 2H, C*H*$(CH_3)_2$), 2.42 (d, $^3J_{H-H}$ = 7 Hz, 2H, CH_2), 1.58 (d, $^3J_{H-H}$ = 7 Hz, 6H, CH(CH_3)$_2$), 1.11 (d, $^3J_{H-H}$ = 7 Hz, 6H, CH(CH_3)$_2$).

$^{13}C\{^1H\}$ NMR ($CDCl_3$, 100 MHz, 25 °C): δ 167.0 (*C*O), 166.2 (N*C*N–Ni), 122.0 (N*C*HCHN), 116.9 (NCH*C*HN), 55.0 (*C*H$_2$), 51.5 (*C*H(CH$_3$)$_2$), 47.2 (*C*H$_2$), 25.6 (CH(*C*H$_3$)$_2$), 20.9 (CH(*C*H$_3$)$_2$). IR data (KBr pellet cm^{-1}): 3434 (w), 3136 (w), 3080 (m), 2952 (w), 2868 (w), 1599 (s), 1462 (w), 1397 (m), 1289 (m), 1240 (m), 1211 (w), 1185 (w), 1134 (w), 969 (w), 948 (w), 776 (w), 698 (w), 685 (w), 608 (w). HRMS (ES): *m/z* 417.1529 [(NHC)Ni+H]$^{+\cdot}$, Calculated 417.1549. Anal. Calc. for $C_{18}H_{26}N_6NiO_2$ (417.13): C, 51.83; H, 6.28; N, 20.15. Found: C, 51.47; H, 6.66; N, 19.87%.

2.6. *N,N′-bis-{[2-(1-benzyl)-imidazolium]acetyl}ethylenediamine dichloride (**3a**)*

N,N′-bis-(2-chloroacetyl)ethylenediamine (1.07 g, 5.02 mmol) and 1-benzylimidazole (1.59 g, 10.0 mmol) were taken in toluene (*ca.* 10 mL) and refluxed overnight to obtain a light brown precipitate, which was isolated by decanting off the solvent. The residue was washed with hot hexane (*ca.* 15 mL) and dried under vacuum to obtain the product **3a** as a light brown powder (2.14 g, 81%). ^1H NMR (DMSO-d_6, 400 MHz, 25 °C): δ 9.50 (s, 2H, NC*H*N), 9.01 (br, 2H, N*H*), 7.83 (s, 2H, NC*H*CHN), 7.78 (s, 2H, NCHC*H*N), 7.45–7.38 (m, 10H, 2C$_6$*H*$_5$), 5.50 (s, 4H, C*H*$_2$), 5.09 (s, 4H, C*H*$_2$), 3.19 (s, 4H, C*H*$_2$). $^{13}C\{^1H\}$ NMR (DMSO-d_6, 100 MHz, 25 °C): δ 165.6 (*C*O), 137.5 (N*C*N), 134.9 (*ipso*-*C*$_6$H$_5$), 129.2 (*o*-*C*$_6$H$_5$), 129.1 (*m*-*C*$_6$H$_5$), 128.6 (*p*-*C*$_6$H$_5$), 124.3 (N*C*HCHN), 122.0 (NCH*C*HN), 52.1 (*C*H$_2$), 51.0 (*C*H$_2$), 38.6 (*C*H$_2$). IR data (KBr pellet cm^{-1}): 3447 (m), 3225 (w), 3064 (m), 2804 (w), 2743 (w), 2677 (w), 2520 (w), 2443 (w), 2056 (w), 1685 (s), 1601 (w), 1560 (s), 1499 (m), 1456 (m), 1364 (w), 1260 (m), 1162 (s), 1085 (m), 1033 (m), 820 (w), 715 (s), 626 (w), 572 (w), 469 (w). HRMS (ES): *m/z* 493.2108 [(NHC)+Cl]$^{+\cdot}$, Calculated 493.2119.

2.7. *{N,N′-bis-{[2-(1-benzyl)-imidazol-2-ylidene]acetyl} ethylenediamine}Ni (**3b**)*

N,N′-bis-{[2-(1-benzyl)-imidazolium]acetyl}ethylenediamine dichloride (0.529 g, 1.00 mmol), $NiCl_2 \cdot 6H_2O$ (0.237 g, 1.00 mmol) and K_2CO_3 (0.417 g, 3.02 mmol) were taken in CH_3CN (*ca.* 30 mL). The reaction mixture was refluxed for 24 h, filtered and the solvent was removed. The residue was extracted in CH_2Cl_2, (*ca.* 20 mL) which was evaporated under vacuum to obtain the product **3b** as a yellow solid (0.329 g, 64%). Single crystal of **3b** was grown by slow evaporation method from a saturated CH_3CN solution. ^1H NMR (DMSO-d_6, 400 MHz, 25 °C): δ 7.39–7.35 (m, 10H, 2C$_6$*H*$_5$), 7.27 (br, 2H, NC*H*CHN), 7.26 (br, 2H, NCHC*H*N), 4.87 (d, $^2J_{H-H}$ = 15 Hz, 2H, C*H*$_2$), 4.41 (d, $^2J_{H-H}$ = 15 Hz, 2H, C*H*$_2$), 4.37 (d, $^2J_{H-H}$ = 15 Hz, 2H, C*H*$_2$), 4.26 (d, $^2J_{H-H}$ = 15 Hz, 2H, C*H*$_2$), 3.67 (d, $^3J_{H-H}$ = 7 Hz, 2H, C*H*$_2$), 2.03 (d, $^3J_{H-H}$ = 7 Hz, 2H, C*H*$_2$). $^{13}C\{^1H\}$ NMR (DMSO-d_6, 100 MHz, 25 °C): δ 166.3 (*C*O), 166.0 (N*C*N–Ni), 136.9 (*ipso*-*C*$_6$H$_5$), 128.7 (*o*-*C*$_6$H$_5$), 127.7 (*m*-*C*$_6$H$_5$), 126.7 (*p*-*C*$_6$H$_5$), 122.7 (N*C*HCHN), 122.5 (NCH*C*HN), 54.2 (*C*H$_2$), 52.5 (*C*H$_2$), 46.9 (*C*H$_2$). IR data (KBr pellet cm^{-1}): 3445 (m), 3087 (w), 2853 (w), 1682 (s), 1574 (s), 1403 (m), 1292 (m), 1251 (w), 1173 (w), 1078 (w), 756 (w), 719 (w), 624 (w). HRMS (ES): *m/z* 513.1533 [(NHC)Ni+H]$^{+\cdot}$, Calculated 513.1549. Anal. Calc. for $C_{26}H_{26}N_6NiO_2 \cdot CH_2Cl_2$ (598.15): C, 54.22; H, 4.72; N, 14.05. Found: C, 54.66; H, 5.14; N, 13.73%.

3. Computational methods

Density functional theory calculations were performed on the three nickel complexes of N-heterocyclic carbenes, **1b–3b** using GAUSSIAN 03 [19] suite of quantum chemical programs. The Becke three parameter exchange functional in conjunction with Lee–Yang–Parr correlation functional (B3LYP) has been employed in this study [20,21]. The LANL2DZ basis set was used for the Ni atom [22] while all other atoms are treated with 6-31G(d) basis set [23]. All stationary points are characterized as minima by evaluating Hessian indices on the respective potential energy surfaces. Tight SCF convergence (10^{-8} a.u.) was used for all calculations.

Inspection of the metal–ligand donor–acceptor interactions was carried out using the charge decomposition analysis (CDA) [24]. CDA is a valuable tool in analyzing the interactions between molecular fragments on a quantitative basis, with an emphasis on the electron donation [25]. The orbital contributions in the NHC–Ni complexes, **1b–3b**, can be divided into two parts:

(i) σ-donation from the NHC → Ni fragment and
(ii) π-back donation from NHC ← Ni fragment

The CDA calculations are performed using the program AOMIX [26] using the B3LYP/LANL2DZ, 6-31G(d) wave function. Molecular orbital (MO) compositions and the overlap populations were calculated using the AOMIX Program. The analysis of the MO compositions in terms of occupied and unoccupied fragment orbitals (OFOs and UFOs, respectively), construction of orbital interaction diagrams, the charge decomposition analysis (CDA) were performed using the AOMIX-*CDA* [27].

4. Biomedical application studies

4.1. Cell culture

Human cervical carcinoma (HeLa), Human breast cancer cells (MCF-7) and Chinese Hamster Ovary (CHO) cells were cultured in Eagle's Minimal Essential Medium (Himedia, Mumbai) supplemented with 10% fetal bovine serum, 2.2 g/L $NaHCO_3$ and 1% antibiotic–antimycotic solution (Himedia, Mumbai) containing streptomycin, amphoterecin B and penicillin. For MCF-7 cells, the medium was supplemented with 0.280 IU of insulin per mL of media. The cells were grown at 37 °C in a humidified atmosphere of 5% CO_2 and 95% air. For cell proliferation assays, cells were seeded at a density of 1×10^5 cells/mL on 96 well plates. For microscopic studies, 0.6×10^5 cells/mL were grown as monolayer

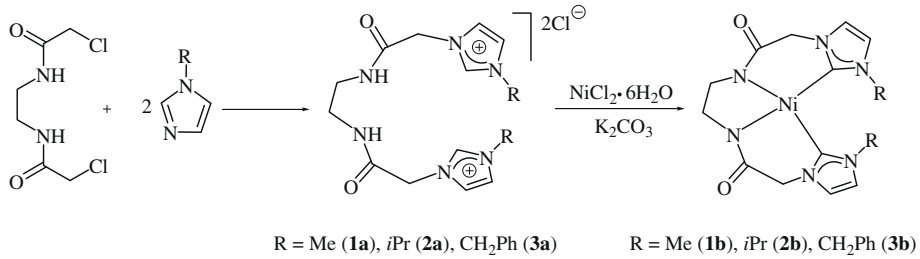

Scheme 1.

on glass cover slips. A solution of following compounds, $NiCl_2 \cdot 6H_2O$, **1a**, **1b**, **2a**, **2b**, **3a** and **3b** in DMSO (0.1% final concentration) were added to the culture medium 24 h after the seeding.

4.2. Cell proliferation

HeLa and MCF-7 cells (1×10^5/mL) were seeded on 96 well plates and grown in the absence and presence of different concentrations (1 μM, 5 μM and 20 μM) of $NiCl_2 \cdot 6H_2O$, **1a**, **1b**, **2a**, **2b**, **3a** and **3b** at 37 °C for one cell cycle. The effects of these compounds on the proliferation of HeLa and MCF-7 cells were determined using a standard sulforhodamine B assay [28]. Non-tumorigenic CHO cells (1×10^5/mL) were seeded on 96 well plates and grown in the presence and absence of $NiCl_2 \cdot 6H_2O$, **3a** and **3b**. To see the effect of sequential addition of reaction components to form the functional nickel complex (**3b**) inside the CHO cells, the $NiCl_2 \cdot 6H_2O$ was added (1, 5, 20 μM) to CHO cells already seeded at a density of 1×10^5 cells/mL. After 1 h, Cs_2CO_3 was added (1, 5, 20 μM) followed by the ligand **3a**. The cells were incubated at 37 °C in a humidified atmosphere of 5% CO_2 and 95% air. Data were the average of two independent experiments.

4.3. Differential interference contrast microscopy (DIC)

The effect of $NiCl_2 \cdot 6H_2O$, **3a** and **3b** on the morphology of HeLa cells was analyzed by DIC microscopy. The cells (0.6×10^5 cells/mL) seeded on glass cover slips were exposed to different concentrations (1, 5 and 20 μM) of the compounds and were examined with a Nikon Eclipse 2000-U microscope and the images were analyzed with image-Pro Plus software.

5. Results and discussion

With the objective of completely engulfing the nickel center, a new class of tetradentate ligand namely, {*N,N'-bis*-{[2-(1-R)-imidazol-2-ylidene]acetyl}ethylenediamine} [R = Me (**1a**), *i*Pr (**2a**), CH_2Ph (**3a**)], was designed. Also, polar amido groups were chosen as N-substituents with the intention of making the nickel complexes water soluble. It was conceived that the tetradentate ligand containing two strongly σ-donating carbene moieties and two polar amido moieties would effectively encapsulate the

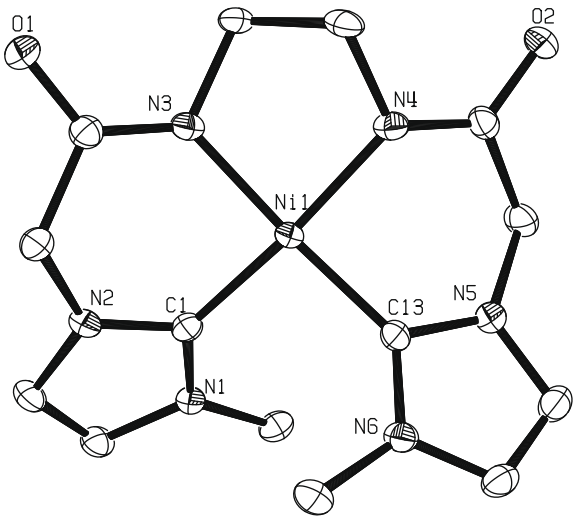

Fig. 2. ORTEP of **1b**. Selected bond lengths (Å) and angles (°): Ni1–C1 1.8670(19), Ni1–C13 1.8590(18), Ni1–N3 1.8913(16), Ni1–N4 1.8982(16), C1–Ni1–C13 95.31(8), C1–Ni1–N3 90.52(7), C13–Ni1–N4 89.95(7), N3–Ni1–N4 85.46(7).

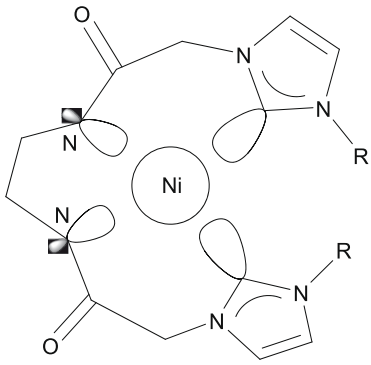

R = Me (**1b**), *i*Pr (**2b**), CH_2Ph (**3b**)

Fig. 3. Interaction of the filled carbene lone pairs and the amido groups of the free NHC ligand fragment with the unfilled 4s orbital of nickel in **1b**–**3b**.

Table 1
Activity of $NiCl_2 \cdot 6H_2O$ and Ni complexes **1b**–**3b** and their corresponding ligands for HeLa cells.

Compound	Inhibition at concentration (μM)[a]		
	1	5	20
$NiCl_2 \cdot 6H_2O$	22	40	86
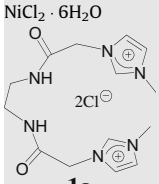 **1a**	0	18	39
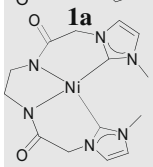 **1b**	6	14	42
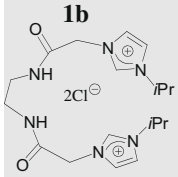 **2a**	0	28	48
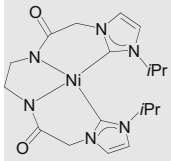 **2b**	0	8	30
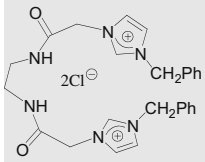 **3a**	0	0	0
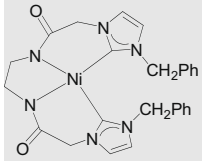 **3b**	0	9	22

[a] Data are the average of two independent experiments.

nickel metal as favored by the entropy driven chelation process and, thus, was anticipated to suppress the high cytotoxicity of the bare nickel ion.

The nickel complexes, **1b–3b** were synthesized from the respective imidazolium dichloride salts, **1a–3a**, by the direct reaction with $NiCl_2 \bullet 6H_2O$ in presence of K_2CO_3 as a base in 64–66% yield (Scheme 1). The distinctive metal bound carbene ($C_{carbene}$–Ni) resonances appeared at 166.7 ppm (**1b**), 166.2 ppm (**2b**), and 166.0 ppm (**3b**) in the $^{13}C\{^1H\}$ NMR spectrum. Interestingly, the amido-NH protons were conspicuously absent in the ^1H NMR spectrum, which not only indicated their deprotonation during the reaction but also suggested the coordination of the amido groups to the metal. The ligand precursors, **1a–3a**, were synthesized by alkylation of the respective imidazoles with *N,N′-bis*-(2-chloroacetyl)ethylenediamine in 55–81% yield (Scheme 1).

In order to check the stability of the nickel complexes in water, we recorded the ^1H NMR spectra in D_2O, which closely resembled the spectra obtained in DMSO-d_6. The water stable nature of **1b–3b** is important particularly with regard to their utility in biomedical application studies. It is worth noting that though a few chelated nickel N-heterocyclic complexes are known, very little information pertaining to their water stability [29], an important criterion for biomedical application studies, exist in the literature.

Indeed, in the molecular structures of **1b–3b**, total chelation of the nickel center through tetradentate binding of the N-heterocyclic carbene ligands were observed (Fig. 2 and see Supplementary Supporting Information Figs. S1, S2 and Table S1). The geometry around the nickel center was found to be distorted square planar with the $C_{carbene}$–Ni distances being 1.8670(19) Å and 1.8590(18) Å in **1b**, 1.870(3) Å in **2b** and 1.8644(15) Å and 1.8637(16) Å in **3b**.

The tight binding of the dianionic {*N,N′-bis*-{[2-(1-R)-imidazol-2-ylidene]acetyl}ethylenediamine} [R = Me, *i*Pr, CH_2Ph] to nickel(II) center was evident by large reduction in computed atomic charges (both in Natural charge as well as Mulliken charge values) at the nickel center in **1b–3b** relative to that of bare nickel(II) ion upon binding of the free NHC ligand fragment on to the metal (see Supplementary Supporting Information, Tables S5–S7). The binding of the NHC ligand fragment to the metal center also leads to significant increase in *3d* and *4s* orbital population as the electronic configuration of nickel(II) center changed from $3d^{8.0}\ 4s^{0}$ in free Ni(II) ionic state to $3d^{8.9}\ 4s^{0.4}$ in **1b–3b** (see Supplementary Supporting Information, Table S8). The NBO Analysis of the Ni–$C_{carbene}$ interaction revealed that the Ni–$C_{carbene}$ bond was composed of an interaction between the sp^2 $C_{carbene}$ orbital and the *sd* orbital of the Ni^{2+} ion (see Supplementary Supporting Information, Table S9). Furthermore, the Charge Decomposition Analysis (CDA) performed on Ni–$C_{carbene}$ interaction of the **1b–3b** complexes revealed that the Ni–NHC interaction comprised of (NHC $\xrightarrow{\sigma}$ Ni) σ-donation, denoted as *d* and an (NHC $\xrightarrow{\pi}$ Ni) π-back donation represented by *b*. It is worth noting that both the (NHC $\xrightarrow{\sigma}$ Ni) σ-donation and the (NHC $\xrightarrow{\pi}$ Ni) π-back donation comprised of two separate interactions, namely, a Ni–$C_{carbene}$ interaction, and an Ni–amido-N^- interaction. Thus, the high *d*/*b* ratios of 9.46 (**1b**), 9.02 (**2b**) and 9.65 (**3b**) suggest the strongly σ-donating nature of the N-heterocyclic carbene ligands in the **1b–3b** complexes (see Supplementary Supporting Information, Table S10). Indeed, a careful look at the simplified molecular orbital correlation diagrams of

Table 2
Activity of $NiCl_2 \cdot 6H_2O$ and Ni complexes **1b–3b** and their corresponding ligands for MCF-7 cells.

Compound	Inhibition at concentration (μM)[a]		
	1	5	20
$NiCl_2 \cdot 6H_2O$	77	90	100
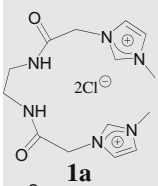 **1a**	0	0	17
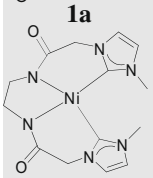 **1b**	6	16	30
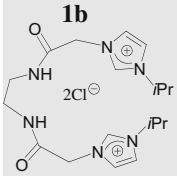 **2a**	0	4	23
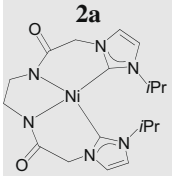 **2b**	0	0	11
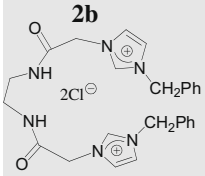 **3a**	0	0	7
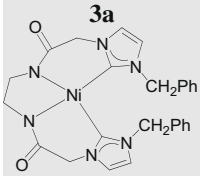 **3b**	0	0	19

[a] Data are the average of two independent experiments.

Table 3
Activity of $NiCl_2 \cdot 6H_2O$ and Ni complex **3b** and its corresponding ligand **3a** for non-tumorigenic CHO cells.

Compound	Inhibition at concentration (μM)[a]		
	1	5	20
$NiCl_2 \cdot 6H_2O$	22	36	76
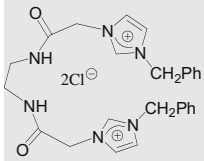 **3a**	6	19	27
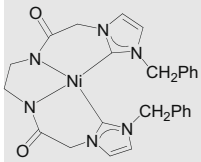 **3b**	13	24	35

[a] Data are the average of two independent experiments.

1b–**3b**, constructed to understand the binding of the NHC ligand fragment with the metal center, reveal that the carbene lone pairs along with the amido groups of the free NHC ligand fragment interacted with the unfilled *4s* orbital of nickel center (Fig. 3 and see Supplementary Supporting Information Figures S3–S5). This overall interaction of the NHC ligand with the nickel based orbital can be observed in the following orbitals, HOMO-22 (**1b**), HOMO-26 (**2b**) and HOMO-32 (**3b**). As these NHC–nickel σ-bonding molecular orbitals are deeply buried, they essentially contribute to the inert nature of the NHC–nickel interaction, which in turn causes the exceptional stability of these complexes.

Quite significantly, the biomedical application studies carried out on **1b**–**3b** relative to that of the $NiCl_2 \cdot 6H_2O$ showed that **1b–3b** exhibited remarkably reduced cytotoxic activity compared to that of $NiCl_2 \cdot 6H_2O$ under analogous conditions. Specifically, cell proliferation studies carried out at three different concentrations (1, 5 and 20 μM) in presence of **1b–3b** on two commonly available human cancer cell lines namely, HeLa and MCF-7 cell lines in culture, showed significant reduction of the cytotoxic activity [(16–64%) for HeLa cells and (70–90%) for MCF-7 cells] for all the nickel complexes in both the cell lines (see Tables 1 and 2). It is worth noting that the significant reduction of the cytotoxic properties of **1b**–**3b**, compared to that of otherwise very toxic Ni(II) ion in $NiCl_2 \cdot 6H_2O$ is brought about by successful chelation of the nickel center in these complexes by the strongly σ-donating tetradentate N-heterocyclic carbene ligands. More interestingly, owing to its

Table 4
Activity of $NiCl_2 \cdot 6H_2O$, and $NiCl_2 \cdot 6H_2O$ followed by Cs_2CO_3[a] and ligand **3a**[a] for non-tumorigenic CHO cells.

Compound	Inhibition at concentration (μM)[b]		
	1	5	20
$NiCl_2 \cdot 6H_2O$	22	36	76
Cs_2CO_3	0	0	0
$NiCl_2 \cdot 6H_2O + Cs_2CO_3 +$ 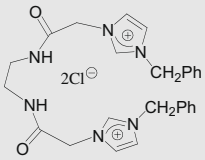 **3a**	29	38	79

[a] The ligand **3a** and Cs_2CO_3 were added after 1 h of the exposure of CHO cells to $NiCl_2 \cdot 6H_2O$.
[b] Data are the average of two independent experiments.

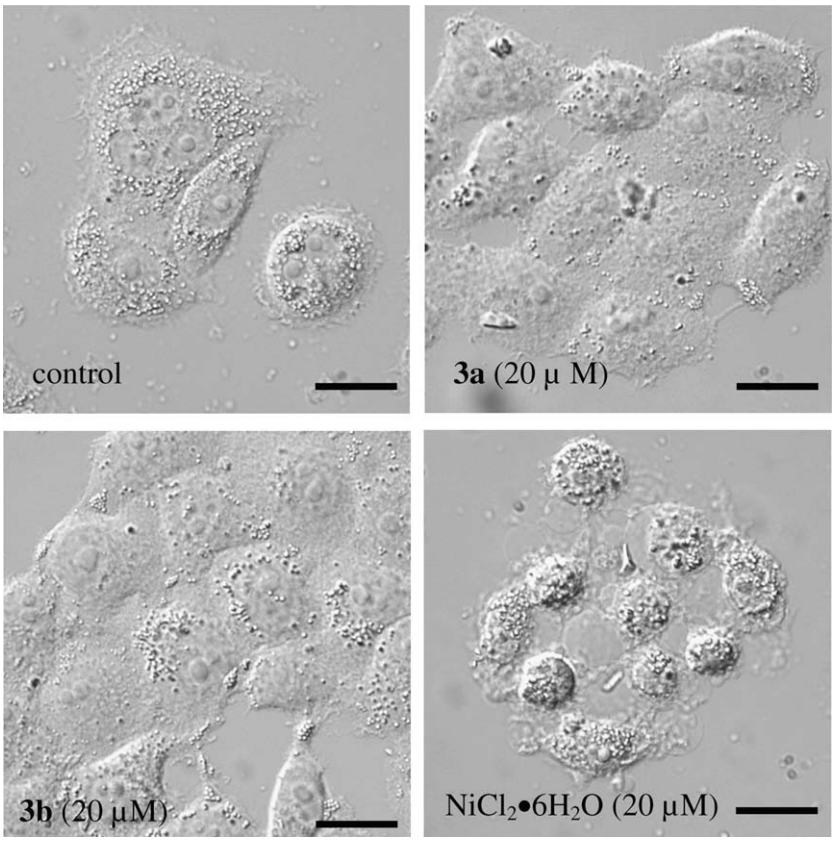

Fig. 4. Effect of ligand **3a**, nickel complex **3b** and $NiCl_2 \cdot 6H_2O$ on the morphology of HeLa cells at 20 μM concentration. Scale bar represents 10 μm.

subdued cytotoxic properties, these complexes, **1b**–**3b**, may find utility as agents for developing resistance to nickel toxicity.

Experiments similar to the effect of $NiCl_2 \cdot 6H_2O$, NHC ligands and the nickel complexes on HeLa and MCF-7 cells were repeated on non-tumorigenic CHO cells by employing a representative ligand **3a** and its nickel complex **3b** (Table 3). The results showed no difference in selectivity of these compounds towards tumorigenic and non-tumorigenic cells. For example, $NiCl_2 \cdot 6H_2O$ exhibited similar cytotoxicity in CHO cells as compared to HeLa and MCF-7 cells and its cytotoxicity decreased when complexed with the NHC ligand.

Further experiments were carried out in order to examine the ability of the NHC ligand to suppress the cytotoxicity arising out of Ni(II) species. Specifically, when the non-tumorigenic CHO cells were exposed to $NiCl_2 \cdot 6H_2O$ for 1 h followed by subsequent addition of the ligand **3a** in presence of Cs_2CO_3, similar cytotoxic effect as compared to $NiCl_2 \cdot 6H_2O$ on CHO cells were observed at all concentrations, thereby suggesting that the sequential addition of the reactants, **3a** and $NiCl_2 \cdot 6H_2O$ in the presence of Cs_2CO_3, failed to result in the intracellular complex (**3b**) formation (Table 4). The observed cytotoxicity in the experiment was very similar to that of $NiCl_2 \cdot 6H_2O$. In this regard, it is worth noting that all of the nickel complexes **1b**–**3b** were synthesized under harsher refluxing conditions as compared to the mild cellular conditions. The control experiment using only Cs_2CO_3 showed that it has no cytotoxic effect on CHO cells at all concentrations.

In order to directly observe the effect of the nickel on the cancer cell lines, morphological studies were carried out using differential interference contrast (DIC) microscopy. In particular, the experiments, which were carried out at three different concentrations (1, 5 and 20 μM) on HeLa cells in presence of $NiCl_2 \cdot 6H_2O$, a representative nickel complex **3b** and its ligand, **3a**, showed that while severe blebbing (erupted spots) for the dying cells were observed in case of $NiCl_2 \cdot 6H_2O$, no such surface abnormalities were seen in case of the representative nickel complex **3b** and its ligand, **3a** (see Fig. 4 and Supplementary Supporting Information Figs. S6 and S7). These observations further substantiate the fact that drastic reduction in the cytotoxic activity of nickel was successfully achieved by encapsulation of the metal center in **1b**–**3b** by employing a new class of tightly binding N-heterocylic carbene ligand.

6. Conclusions

In summary, a series of nickel complexes, **1b**–**3b**, displaying significantly subdued cytotoxic activity towards two commonly available human cancer cell lines namely, HeLa cells and MCF-7 cells, and one non-tumorigenic cell line, CHO cells, in culture as compared to the maximum inhibition by $NiCl_2 \cdot 6H_2O$ under analogous conditions, have been designed. Furthermore, morphological studies on HeLa cells showed that a representative complex, **3b**, caused minimum surface abnormality on the cancer cells consistent with its reduced cytotoxic activity.

Acknowledgements

We thank DST, New Delhi, for financial support of this research. We are grateful to the National Single Crystal X-ray Diffraction Facility and Sophisticated Analytical Instrument Facility at IIT Bombay, India, for the crystallographic and other characterization data. Computational facilities from the IIT Bombay Computer Center are gratefully acknowledged. DP is a Swarnjayanti Fellow. SR thanks Mr. G. N. Gururaja for assistance with the 2D experiments. SR and JA thank CSIR-UGC, New Delhi for research fellowship. JMT thanks National Science Foundation (NSF) Grant No: 0521237 (JMT P.I.) for crystallographic work.

Appendix A. Supplementary data

CCDC 658169, 672002 and 666890 contain the supplementary crystallographic data for **1b**, **2b** and **3b**. These data can be obtained free of charge from The Cambridge Crystallographic Data Centre via www.ccdc.cam.ac.uk/data_request/cif. Supplementary data associated with this article can be found, in the online version, at doi:10.1016/j.jorganchem.2009.03.036.

References

[1] (a) E. Denkhaus, K. Salnikow, Crit. Rev. Oncol./Hematol. 42 (2002) 35;
(b) M.A. Zoroddu, L. Schinocca, T. Kowalik-Jankowska, H. Kozlowski, K. Salnikow, M. Costa, Environ. Health Perspect. 110 (2002) 719.
[2] (a) K. Salnikow, A. Zhitkovich, Chem. Res. Toxicol. 21 (2008) 28;
(b) L. Morgan, V. Usher, Ann. Occup. Hyg. 38 (1994) 189;
(c) D. Akers, R. Dospoy, Fuel Process. Technol. 39 (1994) 73.
[3] C.M. Teaf, B.J. Tuovila, E.J. Zillioux, A. Shipp, G. Lawrence, C. Van Landingham, HERA 10 (2004) 665.
[4] P.J. Blower, Annu. Rep. Prog. Chem. 100 (2004) 633.
[5] (a) F. Leclercq, M. Cohen-Ohana, N. Mignet, A. Sbarbati, J. Herscovici, D. Scherman, G. Byk, Bioconjugate Chem. 14 (2003) 112;
(b) H.-J. Weinmann, R.C. Brasch, W.-R. Press, G.E. Wesbey, Am. J. Roentgenol. 142 (1984) 619.
[6] (a) W. Qu, K.S. Kasprzak, M. Kadiisk, J. Liu, H. Chen, A. Maciag, R.P. Mason, M.P. Waalkes, Toxicol. Sci. 63 (2001) 189;
(b) R.C. Panzani, D. Schiavino, E. Nucera, S. Pellegrino, G. Fais, G. Schinco, G. Patriarca, Int. Arch. Allergy Immunol. 107 (1995) 251;
(c) I.M. Van Hoogstraten, C. Boos, D. Boden, M.E. Von Blomberg, R.J. Scheper, G. Kraal, J. Invest. Dermatol. 101 (1993) 26;
(d) X.W. Wang, R.J. Imbra, M. Costa, Cancer Res. 48 (1988) 6850.
[7] A.T.Y. Lau, J. Zhang, J.-F. Chiu, Toxicol. Appl. Pharmacol. 215 (2006) 1.
[8] C.-C. Lee, W.-C. Ke, K.-T. Chan, C.-L. Lai, C.-H. Hu, H.M. Lee, Chem. Eur. J. 13 (2007) 582.
[9] T. Schaub, U. Radius, Chem. Eur. J. 11 (2005) 5024.
[10] (a) S. Sujith, E.K. Noh, B.Y. Lee, J.W. Han, J. Organomet. Chem. 693 (2008) 2171;
(b) W.-F. Li, H.-M. Sun, M.-Z. Chen, Q. Shen, Y. Zhang, J. Organomet. Chem. 693 (2008) 2047;
(c) W. Buchowicz, A. Kozioł, L.B. Jerzykiewicz, T. Lis, S. Pasynkiewicz, A. Pecherzewska, A. Pietrzykowski, J. Mol. Catal. A 257 (2006) 118;
(d) B.E. Ketz, X.G. Ottenwaelder, R.M. Waymouth, Chem. Commun. (2005) 5693.
[11] J. Wolf, A. Labande, M. Natella, J.-C. Daran, R. Poli, J. Mol. Catal. A 259 (2006) 205.
[12] W.-H. Yang, C.-S. Lee, S. Pal, Y.-N. Chen, W.-S. Hwang, I.J.B. Lin, J.-C. Wang, J. Organomet. Chem. 693 (2008) 3729.
[13] (a) M.K. Samantaray, K. Pang, M.M. Shaikh, P. Ghosh, Dalton Trans. (2008) 4893;
[b] M.K. Samantaray, K. Pang, M.M. Shaikh, P. Ghosh, Inorg. Chem. 47 (2008) 4153;
(c) L. Ray, M.M. Shaikh, P. Ghosh, Inorg. Chem. 47 (2008) 230;
(d) M.K. Samantaray, D. Roy, A. Patra, R. Stephen, M. Saikh, R.B. Sunoj, P. Ghosh, J. Organomet. Chem. 691 (2006) 3797.
[14] S. Ray, R. Mohan, J.K. Singh, M.K. Samantaray, M.M. Shaikh, D. Panda, P. Ghosh, J. Am. Chem. Soc. 129 (2007) 15042.
[15] (a) L. Ray, S. Barman, M.M. Shaikh, P. Ghosh, Chem. Eur. J. 14 (2008) 6646;
(b) L. Ray, V. Katiyar, S. Barman, M.J. Raihan, H. Nanavati, M.M. Shaikh, P. Ghosh, J. Organomet. Chem. 692 (2007) 4259;
(c) M.K. Samantaray, V. Katiyar, K. Pang, H. Nanavati, P. Ghosh, J. Organomet. Chem. 692 (2007) 1672;
(d) L. Ray, M.M. Shaikh, P. Ghosh, Organometallics 26 (2007) 958;
(e) L. Ray, M.M. Shaikh, P. Ghosh, Dalton Trans. (2007) 4546;
(f) L. Ray, V. Katiyar, M.J. Raihan, H. Nanavati, M.M. Shaikh, P. Ghosh, Eur. J. Inorg. Chem. (2006) 3724;
(g) M.K. Samantaray, V. Katiyar, D. Roy, K. Pang, H. Nanavati, R. Stephen, R.B. Sunoj, P. Ghosh, Eur. J. Inorg. Chem. (2006) 2975.
[16] E. Mas-Marzá, E. Peris, I. Castro-Rodŕiguez, K. Meyer, Organometallics 24 (2005) 3158.
[17] H.M. Lee, C.Y. Lu, C.Y. Chen, W.L. Chen, H.C. Lin, P.L. Chiu, P.Y. Cheng, Tetrahedron 60 (2004) 5807.
[18] (a) G.M. Sheldrick, SHELXL-97, Program for Refinement of Crystal Structures, University of Gottingen, Germany, 1997;
(b) G.M. Sheldrick, SHELXS-97, Structure Solving Program, University of Gottingen, Germany, 1997.
[19] M.J. Frisch et al., Gaussian Inc., Wallingford, CT, 2004.
[20] A.D. Becke, Phys. Rev. A 38 (1988) 3098.
[21] C. Lee, W. Yang, R.G. Parr, Phys. Rev. B 37 (1988) 758.
[22] (a) Q.-Z. Han, Y.-H. Zhao, H. Wen, Data Sci. J. 6 (2007) S837;
(b) D.C. Graham, K.J. Cavell, Brian F. Yates, Dalton Trans. (2007) 4650;
(c) E.B. Kadossov, K.J. Gaskell, M.A. Langell, J. Comput. Chem. 28 (2007) 1240;
(d) K. Cochran, G. Forde, G.A. Hill, L. Gorb, J. Leszczynski, Struct. Chem. 13 (2002) 133.
[23] W.J. Hehre, R. Ditchfield, J.A. Pople, J. Chem. Phys. 56 (1972) 2257.

[24] S. Dapprich, G. Frenking, J. Phys. Chem. 99 (1995) 9352.
[25] (a) S.F. Vyboishchikov, G. Frenking, Chem. Eur. J. 4 (1998) 1439;
(b) G. Frenking, U. Pidun, J. Chem. Soc., Dalton Trans. (1997) 1653.
[26] S.I. Gorelsky, AOMIX: Program for Molecular Orbital Analysis, York University, Toronto, Canada, <http://www.sg-chem.net/>, 1997.
[27] S.I. Gorelsky, S. Ghosh, E.I. Solomon, J. Am. Chem. Soc. 128 (2006) 278.
[28] (a) R. Mohan, M. Banerjee, A. Ray, T. Manna, L. Wilson, T. Owa, B. Bhattacharyya, D. Panda, Biochemistry 45 (2006) 5440;
(b) K.T. Papazisis, G.D. Geromichalos, K.A. Dimitriadis, A.H. Kortsaris, J. Immun. Meth. 208 (1997) 151.
[29] (a) P.L. Chiu, C.-L. Lai, C.-F. Chang, C.-H. Hu, H.M. Lee, Organometallics 24 (2005) 6169;
(b) M.V. Baker, B.W. Skelton, A.H. White, C.C. Williams, Organometallics 21 (2002) 2674;
(c) M.V. Baker, B.W. Skelton, A.H. White, C.C. Williams, J. Chem. Soc., Dalton Trans. (2001) 111.